Application of the Electrochemical Impedance Technique to Study of Pillared Clays

J. C. Galván, A. Jiménez-Morales,† R. Jiménez, J. Merino, A. Villanueva, M. Crespin,‡ P. Aranda, and E. Ruiz-Hitzky*

Instituto de Ciencia de Materiales de Madrid, CSIC, Cantoblanco, 28049 Madrid, Spain

Received February 6, 1998. Revised Manuscript Received July 22, 1998

The electrochemical impedance technique combined with other conventional characterization techniques (XRD, NMR, TG, DSC, CRTA, specific surface area and porosity determinations, etc.) has been applied to study the in situ formation of alumina pillared smectite clay materials (Al-PILCs). The main objective of this work is to clarify the mechanism of pillar formation and, simultaneously, to explore the usefulness of the electrochemical impedance technique to correlate experimental conditions (e.g. temperature range) for H^+ generation with the electrical conductivity of the system. It is shown that the changes in the conductivity could be associated with the mobility and/or concentration of the protons formed during the thermal decomposition of the interlayered polyoxyhydroxy cations to the pillar oxide. This study has also been extended to other PILCs prepared either with different clays (e.g. montmorillonite, saponite) or by incorporating oxide pillars of different nature (e.g. alumina, zirconia).

Introduction

Much work has been devoted to develop new nanoporous materials with controlled porosity,[1] in view to their viability for numerous applications in adsorption, catalysis, and separation technologies (sorbents, catalysts, molecular sieves, sensors, and membranes). Among this class of solids, the so-called pillared clays (pillared interlayered clays, PILCs) derived from 2:1 charged phyllosilicates (e.g. smectites) have been investigated since the 1970s.[2−10] More recently, several comprehensive reviews covering a broad variety of topics on PILCs have been published,[11−16] although there is still a significant lack of information related to the formation mechanism of such materials.

Numerous analytical tools (XRD; TEM and SEM; gas adsorption isotherms; thermoanalytical techniques; IR, EPR, solid-state NMR, and Mössbauer spectroscopies) have been used to study the formation of Al-pillared clays (Al-PILCs).[11,12] However, some aspects of the chemistry related to the generation of alumina pillars from intercalated aluminum polyoxyhydroxy cations (i.e., "Al_{13}" Keggin cages) still remain unclear. In agreement with Vaughan and Lussier,[17] and more recently with Schoonheydt et al.,[18,19] it is generally accepted that Al-PILCs are formed by the thermal decomposition of the Al-oxyhydroxy species intercalated in smectites, leading to the alumina pillars. If we consider, for instance, that only the Al_{13} precursor species, $[Al_{13}O_4(OH)_{24}(H_2O)_{12}]^{7+}$, are present in the interlayer region of the silicate before the calcination step, it is assumed that alumina pillars are formed according to eq 1:

$$[Al_{13}O_4(OH)_{24}(H_2O)_{12}]^{7+} \xrightarrow{\Delta} [Al_{13}O_4(OH)_{24+x}(H_2O)_{12-x}]^{(7-x)+} + xH^+$$

$$\downarrow$$

$$\downarrow \Delta$$

$$\downarrow$$

$$13/2\ Al_2O_3 + 20.5\ H_2O + 7\ H^+ \qquad \text{(eq.1)}$$

This equation assumes a model based on the simplistic case of a unique oxyhydroxy-Al species, although it is

* Corresponding author. E-mail: eduardo@icmm.csic.es.
† Present address: Universidad Carlos III de Madrid, Leganés 28911-Madrid, Spain.
‡ Present address: Centre de Recherche sur la Matière Divisée (CNRS) and Université d'Orleans, F-45071 Orléans 2, France.

(1) Pinnavaia, T. J.; Thorpe M. F., Eds. *Access in Nanoporous Materials*; Plenum Press: New York, 1995.
(2) Brindley, G. M.; Sempels, R. E. *Clay Miner.***1977**, *12*, 229.
(3) Lahav, N.; Shani, N.; Shabtai, J. *Clays Clay Miner.* **1978**, *26*, 107.
(4) Vaughan, D. E. W.; Lussier, R. J.; Magee, J. S., Jr. U.S. Patent 4,176,090, 1979.
(5) Shabtai, J.; Lazar, R.; Oblad, A. G. In *Proceedings of the International Congress on Catalysis*; Seiyama, T., Tanabe, K., Eds.; Elsevier: Amsterdam, 1980; p 829.
(6) Occelli, M. L.; Tindwa R. M. *Clays Clay Miner.* **1983**, *31*, 22.
(7) Pinnavaia, T. J. *Science* **1983**, *220*, 365.
(8) Plée, D.; Schutz A., Poncelet, G.; Fripiat J. J. In *Catalysis by Acids and Bases, Studies in Surface Science and Catalysis*; Imelik B., Naccache, C., Coudrier, G., Taarit, Y. B., Vedrine, J. C., Eds.; Elsevier: New York 1985; Vol. 20, p 343.
(9) Plée, D.; Borg, F.; Gatineau L.; Fripiat J. J. *J. Am. Chem. Soc.* **1985**, *107*, 2362.
(10) Schutz, A.; Stone, W. E. E.; Poncelet, G.; Fripiat J. J. *Clays Clay Miner.* **1987**, *35*, 251.
(11) Burch, R., Ed. "Pillared Clays" (Special issue) *Catalysis Today* **1988**, *2*, 18.
(12) Mitchell, I. V., Ed. *Pillared Layered Structures. Current Trends and Applications*; Elservier: London, 1990.
(13) Yang, R. T.; Baksh, M. S. A. *AIChE* **1991**, *37*, 679.
(14) Ohtsuka, K. *Chem. Mater.* **1997**, *9*, 2039.
(15) Lambert J. F.; Poncelet G. *Topics Catal.* **1997**, *4*, 43.
(16) Jones W.; Poncelet, G.; Ruiz-Hitzky, E.; Galván, J. C.; Pomonis, P.; Van Damme, H.; Bergaya, F.; Papayanakos, N.; Gangas, N. *The Synthesis, Characterization and Application of Pillared Clays (PILCs) Produced in Large Quantities.* Synthesis Report for publication. Date 26-10-97. Contract No. BR2-CT-94-0629 EU BRITE/EURAM-II Project No. 8211, 1997.

10.1021/cm980076i CCC: $15.00
Published on Web 10/22/1998

generally admitted that this polycation predominates over other forms of hydroxylated and hydrated Al^{3+} cations that are also present in the Al-PILC precursors (Al-pre-PILCs). However, the formation mechanism of alumina from such species (Al_{13} and eventually other hydrated Al-polyoxyhydroxy cations) may result in similar pillars (mostly alumina) following similar processes involving the loss of water and hydroxyl groups accompanied by the simultaneous release of protons, as the thermal treatment progresses.

As a novelty in the pillared clays investigations, and with the aim to study the formation mechanism of Al-PILCs, we have applied electrochemical impedance spectroscopy (EIS),[20] coupled with other physicochemical characterization methods (XRD, NMR, TG, DSC, CRTA, specific surface area and porosity determinations, etc.). The objective was to follow the changes of the electrical conductivity that could be associated with the changes of the mobility and/or concentration of the protons released during the pillar oxide formation. EIS is a powerful tool widely used to study the electrical and electrochemical properties of a large variety of systems. Electrochemical processes (e.g. metallic corrosion,[21] ion mobility in membranes[22]) and materials (e.g. ion conductors[23]) are examples illustrating the usefulness of the EIS technique.

The present study concerns Al-PILCs derived from well-known 2:1 charged phyllosilicates of the smectite group. They are (1) montmorillonite $[Si_8]^{IV}[Al_{4-x}Mg_x]^{VI}O_{20}(OH)_4(M_{x/n})^{n+}\cdot yH_2O$ (ideal formula), which is a dioctahedral aluminum clay where the layer charge originates from octahedral substitution of Al(III) by Mg(II), and (2) saponite, $[Si_{8-x}Al_x]^{IV}[Mg_6]^{VI}O_{20}(OH)_4(M_{x/n})^{n+}\cdot yH_2O$ (ideal formula), which is a trioctahedral magnesium clay where the layer charge originates from tetrahedral substitution of Si(IV) by Al(III).

Experimental Section

Preparation of Al-PILCs. The SWy-1 montmorillonite (Crook County, Wyoming, obtained from the Source Clay Repository of the Clay Minerals Society, University of Missouri, Columbia), was Na^+-exchanged by washing several times with a 1 M NaCl solution and purified by sedimentation to obtain the $<2\ \mu$m particle size fraction. The homoionic clay was used to prepare the Al-pre-PILCs. The pillaring reagent was prepared by slow addition (1 h) of a 0.4 M solution of NaOH to a 0.4 M solution of $Al(NO_3)_3\cdot\times b09H_2O$, to reach a OH/Al molar ratio of 2.4; the measured pH was 4.8. A typical experimental set consisted in the use of 5 g of Na-montmorillonite (2% aqueous dispersion) that was treated at 80 °C with the aluminum polyoxyhydroxy cation pillaring reagent. Under these conditions the amount of Al per gram of clay used in the preparation is 6.6 mmol·g^{-1}. The mixture was maintained under continuous magnetic stirring at 80 °C for 3 h. The slurry was dialyzed until the nitrate ions were completely eliminated. Finally, the Al-pre-PILC material was recovered by filtration and air-dried at 50 °C. This material was the precursor used to obtain the corresponding Al-PILCs by further thermal treatment (calcination step) carried out in situ in the experimental studies using different techniques.

Other PILCs samples, Al- and Zr-PILCs, were prepared with SWy-1 Wyoming montmorillonite following a similar procedure. Al-PILCs labeled EY for saponite (Yunclillos, Spain; supplied by TOLSA S.A.) were prepared by Poncelet's group at the Catholic University of Louvain, Belgium.[16] Two sets of Al-PILCs were prepared at the kilogram per batch level by Papayanakos' group at the National Technical University of Athens,[16] Greece, derived from acid-activated montmorillonites samples with trade name FULCAT F22B from Laporte, U.K. One such set was prepared from precursors obtained at room temperature (labeled 1C), and a second one after aging the Al pillaring reagent solutions at 80 °C (labeled 1W and 4W).

Characterization. Both pre-PILCs and PILCs were characterized by XRD (Philips PW 1710 Instrument with a Cu anode and Ni filter, and a Siemens apparatus equipped with an Anton PAAR KG high-temperature chamber) and by chemical analysis (EDX, Zeiss, DSM 960). The thermal analyses (TG, DTA, and DSC) were carried out in a SEIKO SSC/5200 model under a continuous flow of dry N_2 (100 mL/min), using alumina as a reference material. The specific surface area and porosity analyses (Coulter, Omnisorp 100 model) and solid-state NMR spectroscopy (Bruker MSL-400) were also used to characterize pre-PILC and PILC materials. Changes with temperature of the residual pressure accompanying the water desorption and dehydroxylation processes were monitored during the in situ synthesis of the Al-PILC in a modified Controlled Rate Thermal Analysis (CRTA) apparatus.[16,24]

Electrochemical Impedance Study. Powders of pre-PILCs were pressed (3 ton/cm^2) into pellets 260−300 μm thick and 13 mm in diameter. The pellets were Au sputtered and subsequently sandwiched between two identical platinum electrodes in a conductivity cell. The impedance measurements were made in the frequency range from 0.1 MHz to 100 mHz with a Solartron 1255 frequency response analyzer coupled to a Princeton Applied Research PAR 273A potentiostat/galvanostat by applying a 100 mV amplitude signal. The impedance spectra were recorded after progressive thermal treatments of pre-PILCs carried out in the temperature range 20−850 °C under N_2 flow. The heating rate during EIS measurements was about 2 °C/min. Thus, the time to reach 450 °C from room temperature was approximately 265 min (i.e. comparable to the duration of a conventional preparation of Al-PILC by the calcination of PILC precursors in a conventional oven). The treatment and simulation of the impedance data were done with a computer program developed by Boukamp.[25]

Results and Discussion

Table 1 shows some physicochemical characteristics of Al-PILC derived from Wyoming montmorillonite obtained as described in the Experimental Section, i.e., by calcination of the corresponding precursor (Al-pre-PILC) in a conventional oven (450 °C, 5 h). These data agree with the typical behavior for this class of porous materials, indicating that the Al-pre-PILCs used in the further experiments generate well-structured Al-PILCs. In situ XRD patterns (Figure 2) obtained during the thermal treatment processes leading to the pillar formation, show a typical shrinkage, from 18.5 to 17.5 Å, accompanying the dehydroxylation of the pillar precursor to the oxide form. The access to the intracrystalline galleries of the pillared materials is revealed by the

(17) Vaughan, D. E. W.; Lussier R. J. In *Proceedings of the Fifth International Conference on Zeolites*; Rees, L. V. C., Ed.; Heyden: London, 1980; p 94.
(18) Schoonheydt, R. A.; Leeman, H. *Clays Clay Miner.* **1992,** *35*, 249.
(19) Schoonheydt, R. A.; Leeman, H.; Scorpion, A.; Lenotte, I.; Grobet, P. J. *Clays Clay Miner.* **1994**, *42*, 518.
(20) Macdonald J. R., Ed. *Impedance Spectroscopy; Emphasizing Solid Materials and Systems;* John Wiley & Sons: New York, 1987. (b) Jonscher A. K. *Dielectric Relaxation in Solids*; Chelsea Dielectrics Press: London, 1983.
(21) Jiménez-Morales, A.; Galván, J. C.; Rodriguez R.; De-Damborenea, J. J. *J. Appl. Electrochem.* **1997**, *27*, 550.
(22) Aranda, P.; Jiménez-Morales, A.; Galván, J. C.; Casal, B.; Ruiz-Hitzky, E *J. Mater. Chem.* **1995**, *5*, 817.
(23) Amarilla, J. M.; Casal, B.; Galván, J. C.; Ruiz-Hitzky, E. *Chem. Mater.* **1992**, *4*, 297.
(24) Rouquerol, J. *J. Therm. Anal.* **1970**, *2*, 123.
(25) Boukamp, B. A. *Manual AC−Immittance Data Analysis System 'Equivalent Circuit'*, Version 4.50, University of Twente: Twente, 1993.

Table 1. Characteristics of the Studied Samples

samples	basal spacing d_{001} (Å)	surface area[a] (m^2/g)	micropore volume[b] (cm^3/g)	maximum effective pore diameter[c] (Å)	SiO_2 content[d] (%)	Al_2O_3 content[d] (%)	Na_2O content[d] (%)
montmorillonite (SWy-1)	12.3	24	0.01		69.7	21.5	1.78
Al-pre-PILC	18.5	295	0.13	7.0	66.0	29.1	0.13
Al-PILC	17.5	297	0.13	7.7	63.6	29.5	0.15

[a] BET, N_2. [b] MP method. [c] Horvarth−Kawazoe method. [d] From EDX analyses.

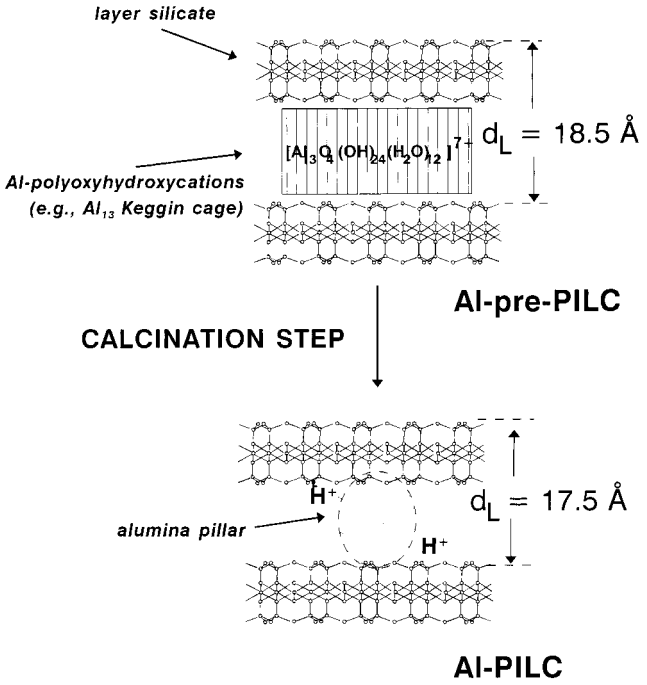

Figure 1. Schematic model representing the calcination step in the Al-pre-PILC.

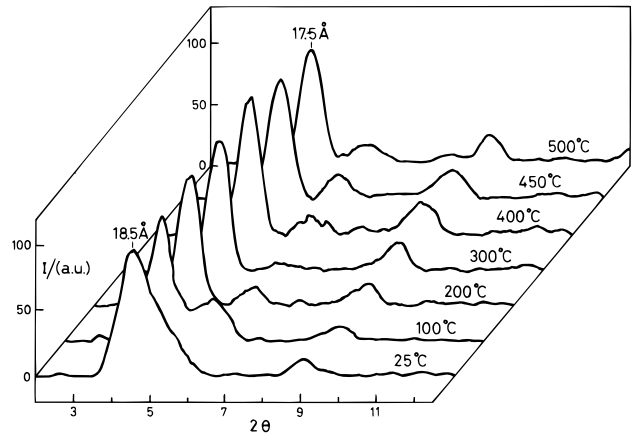

Figure 2. XRD patterns recorded during in situ Al-PILC formation by heating the corresponding precursor (Al-pre-PILC).

Horvarth−Kawazoe analyses,[26] applied to the treatment of the N_2 adsorption isotherms, using the sorptometer to follow the in situ calcination of the Al-pre-PILC by consecutive gas adsorption measurements (Table 2). The maximum effective pore diameters determined from these analyses are in the range 7.0−7.7 Å, which is in agreement with the basal spacings obtained from the XRD patterns. It is important to note that the specific surface area (about 300 m^2/g) and the micropore volume (about 0.15 cm^3/g) remain nearly unvaried during the different steps ascribed to the Al-PILC formation.

Table 2. Specific Surface Area (S_0), Microporous Volume (V_p), and Maximum Effective Pore Diameter ($\varnothing_{HK}$) Measured after Consecutive Thermal Treatments under Reduced Pressure (P) of an Al-pre-PILC Sample

thermal treatments					
T (°C)	time (h)	P ($\times 10^5$ Torr)	S_0[a] ($m^2 \cdot g^{-1}$)	V_P[b] ($cm^3 \cdot g^{-1}$)	$\varnothing_{HK}$[c] (Å)
150	2	3	295	0.13	7.0
200	0.5	7	301	0.13	7.2
250	0.5	7	308	0.14	7.2
300	0.5	7	306	0.17	7.5
350	0.5	3	305	0.14	7.5
400	0.5	2	299	0.13	7.5
450	0.5	10	297	0.13	7.7

[a] BET, N_2. [b] MP. [c] Horvarth−Kawazoe method.

Figure 3 shows the results obtained from the thermal analyses of Al-pre-PILCs during the in situ formation of the corresponding Al-PILCs following a procedure similar to that adopted for the preparation of conventional PILCs (similar heating rate and duration of the thermal treatment). According to these results and taking into account information previously reported by different authors,[27,28] the processes taking place during the thermal treatment of the Al-pre-PILC from room temperature to around 800 °C may be summarized as follows: loss of physically adsorbed water molecules filling the galleries of Al-pre-PILCs, loss of coordinated water molecules belonging to the intercalated Al-polyoxyhydroxy cations, dehydroxylation of the intercalated Al-polyoxyhydroxy cations, proton migration to the octahedral layers, and dehydroxylation of the clay structure.

All of these processes that occur in different temperature ranges can be delimited by using the electrochemical impedance technique combined with the thermal analytical tools. The impedance plot of Al-pre-PILCs recorded at room temperature in an atmosphere of 55% relative humidity exhibits, in the Nyquist representation, a depressed semicircle at high-frequency values and a straight line with a slope close to 1 at low frequencies (Figure 4).[29] The conventional equivalent circuit representing this behavior consists of the association in series of a resistor (R) and a Warburg impedance (Z_W), both in parallel to a constant phase element (CPE).[20,30] The ac response, which defines the semicircle, is dominated by the resistance (R) which, in

(26) Horvath, G.; Kawazoe, K. *J. Chem. Eng. Jpn.* **1983**, *16*, 470.

(27) Pires, J.; Brotas de Carvalho, M.; Carvalho, A. P. *Zeolites* **1997**, *19*, 107.

(28) Pesquera, C.; González, F.; Blanco, C.; Benito, I.; Mendioroz, S. *Thermochim. Acta* **1993**, *219*, 179.

(29) Circuit parameters obtained by simulation: $R = 1.49 \times 10^4$ Ω, $Y_{0,W} = 4.42 \times 10^{-7}\ \Omega^{1-} \cdot s^{1/2}$, $Y_{0,CPE} = 2.19 \times 10^{-7}\ \Omega^{1-} \cdot s^{0.67}$, and $n_{CPE} = 0.67$. The description codes of these equivalent circuit elements are given by Boukamp in ref 25. The total ion conductivity can be calculated by using eq 2: $\sum \sigma_i = 1.34 \times 10^{-6}\ S \cdot cm^{-1}$, being $l/A = 0.02$.

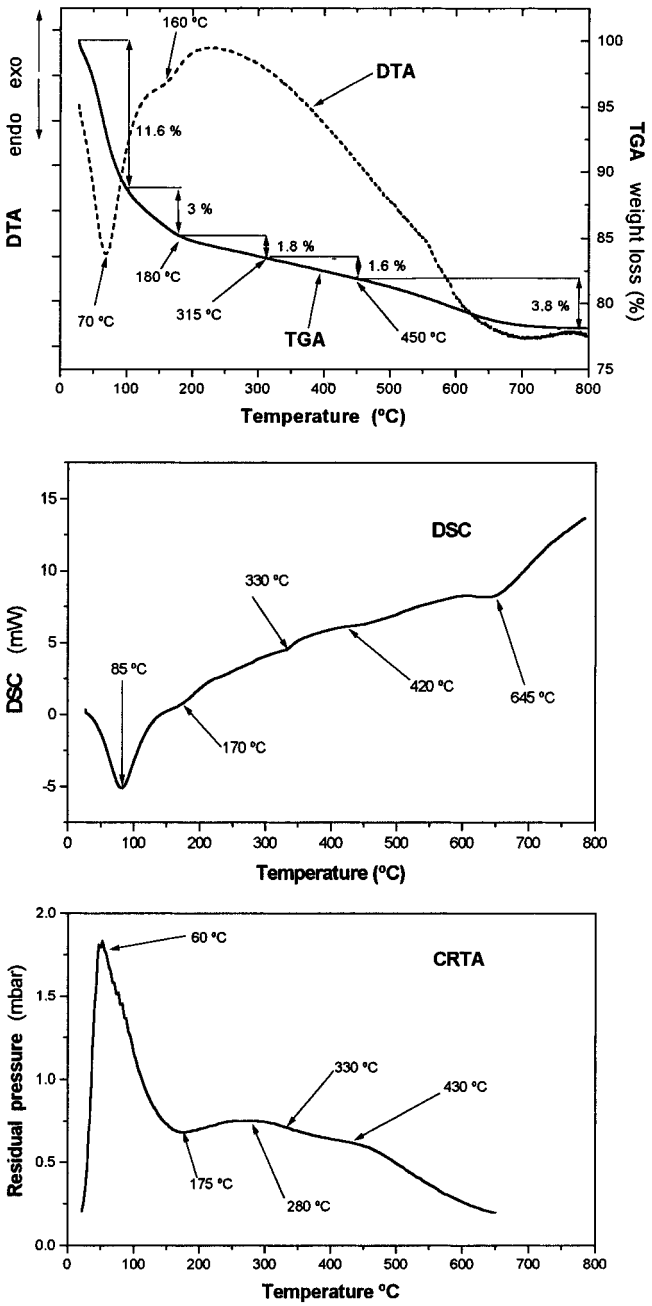

Figure 3. Thermal analyses (TG, DTA, DSC, and CRTA) carried out during the in situ formation of Al-PILCs.

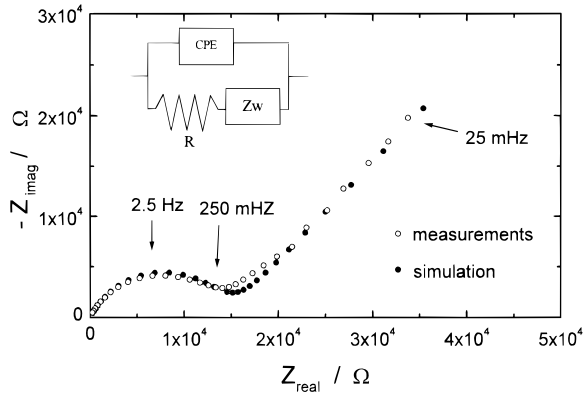

Figure 4. Experimental and simulated impedance Nyquist plots and proposed equivalent circuit for an Al-pre-PILC sample measured at 20 °C and 55% relative humidity (see the values of the circuit parameters in ref 29).

turn, depends on the total ion conductivity, $\sum\sigma_i$ (i.e. the mobility and concentration of all the ions present in the material)

$$R = \frac{1}{\sum_i \sigma_i} \frac{l}{A} \tag{2}$$

where l is the length (cm) of the sample, A is the cross-sectional area (cm^2), and σ_i is the partial ion conductivity of mobile species i ($ohm^{-1}\cdot cm^{-1}$) and

$$\sigma_i = n_i|z_i|e\mu_i \tag{3}$$

where n_i is the number of charge carriers i, per cm^3, z_i is its valence, e is the unit charge (1.60×10^{-19} C), and μ_i is the mobility of these charge carriers i ($cm^2/V\cdot s$).

The ion conductivity of the Al-pre-PILCs measured at room temperature can be ascribed to the transport of the electrical signal by mobile ionic species (ions/protons). The nature of these ionic species could be related to both remaining exchangeable Na^+ ions and hydrated Al^{3+} and/or small Al-polymeric forms (dimers, etc.), but their contribution to conductivity should be limited compared to that of H^+ originating from the high degree of dissociation of water molecules located near the Al^{3+}-oxyhydroxy entities in the interlayer region.[15]

From inspection of eq 3, we find that the conductivity of materials can change either by (i) controlling the mobility—or ease of movement—of the charge carriers, or (ii) controlling the number of charge carriers in the material. In our case, the changes of conductivity will be mainly due to both the proton mobility changes produced by thermal activation and the concentration changes of protons generated in the Al-pre-PILC during the thermal treatment used to obtain the corresponding Al-PILCs (eq 2).

When the sample is heated under a flow of dry nitrogen, the impedance spectra drastically change, showing larger semicircles as temperature increases (Figure 5), indicating a decrease of the electrical conductivity (i.e. an increase of the value of the resistance component). This behavior is observed in the here-called temperature range A (Figure 6) (i.e. for thermal

(30) At low frequencies the impedance plot exhibits a linear region which is inclined at an angle of 45° to the real axis, which is assigned to some form of mass transport of Warburg diffusive type (Z_W) due to a concentration gradient within the material (Figure 4).[20] This situation appears when the material contains more than one mobile species, one of which is electroactive while at least one of the other ionic species has a greater transport number (see for instance the following reference: Bruce, P. G. In *Polymer Electrolyte reviews-1*; MacCallum, J. R., Vincent, C. A., Eds.; Elsevier Applied Science: London, 1987; p 237−274). Although it is possible to explain a plot consisting of a semicircle followed by a spike in terms of a simple equivalent circuit with a resistor R associated in series with the Warburg impedance (Z_W) and both associated in parallel to an ideal capacitor C, to account for the flattening of the semicircle requires the use of a constant phase element CPE (Figure 4),[20] which takes into account the polarization increment and the variation of the dielectric parameters with frequency. Physically, this parameter can be thought of as having characteristics intermediate between a capacitor and a resistor. The ac response of the CPE is described by an empirical impedance function of the type $Z(\omega) = 1/Y_o(j\omega)^n$, where j is the imaginary number ($j^2 = -1$), Y_o is the CPE constant ('S'), ω is the angular frequency ($rad\cdot s^{-1}$), $n = \alpha/(\pi/2)$ is the CPE power, and α is the phase angle of the CPE. The factor n is an adjustable parameter that usually lies between 0.5 and 1. The CPE only describes an ideal capacitor when $n = 1$. Otherwise, for $0.5 < n < 1$, the CPE describes a distribution of dielectric relaxation times in frequency space.

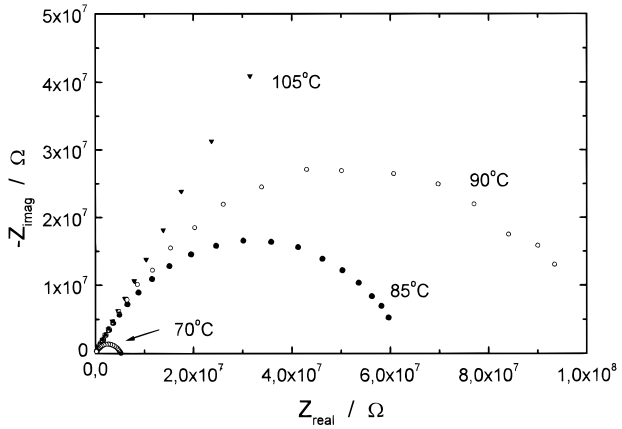

Figure 5. Nyquist plots obtained for different temperature during thermal treatment of an Al-pre-PILC.

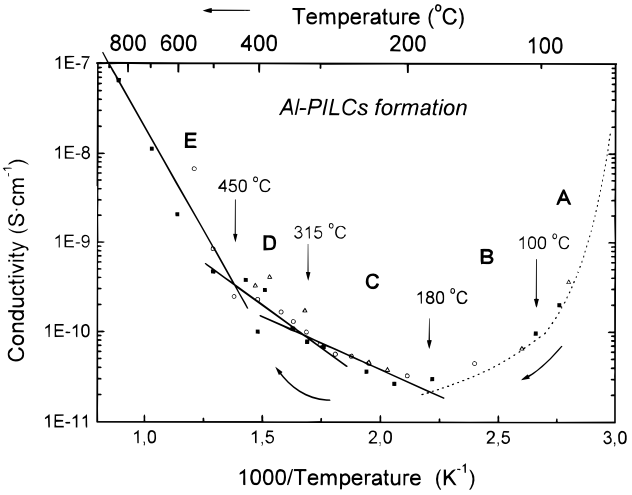

Figure 6. Conductivity values for different Al-**pre**-PILC samples (■, △, ○), obtained from impedance measurements in the temperature range 25−850 °C.

treatments ≤100 °C), and it is consistent with the loss of the physically adsorbed water molecules present on the Al-pre-PILC surface (11.6% as indicated by the TG curve). Thus, the ion-conductivity diminishes as the content of water molecules, acting as carriers for the charged species, progressively diminishes. In this temperature domain the conductivity could be mainly associated also with protons present in the interlayer region of the silicate. In this context, Lambert and Poncelet, in a recent review,[15] show some evidence establishing the reality of the presence of protons originating from dissociated water molecules occurring in hydrated systems as the Al_{13} precursor species and at temperatures as low as and even below 100 °C.

Above 100 °C, an decrease in the electrical conductivity is observed, although fewer time-dependent processes occur at such temperatures. This general behavior of Al-pre-PILCs is illustrated in Figure 6. The region taking place between approximately 100 and 180 °C (temperature range B) may be ascribed to the loss of water molecules coordinated to intercalated Al-polyoxyhydroxy interlayer cations. The conductivity is practically constant in this temperature interval and reaches its lowest values due to the progressive removal of the water molecules (3% weight loss from TG data), which were acting as support for the mobile ions (mainly protons). More precisely, it can be remarked from the DTA and DSC thermal analyses (Figure 3) that one endothermic process occurs in the range 160−170 °C. The CRTA experiments indicate a significant change of the thermal behavior from about 175 °C (Figure 3). This process is directly related with the change of the impedance behavior described above.

As thermal treatment progresses from 180 to 315 °C, a linear increase of the electrical conductivity with the temperature is clearly observed (region C in Figure 6). This increase of the conductivity could be associated with the generation of H^+ species during the formation of the alumina pillars (eq 1). In this conductivity region, the calculated activation energy has relatively low values (0.2 eV). In this temperature range, a set of processes that can mainly be ascribed to the loss of water (1.8% from the TG data) coming from the condensation of hydroxyls belonging to the intercalated Al-polyoxyhydroxy species leads to generation of protons. Simultaneously, the CRTA curve in this temperature interval (Figure 3) presents a large band with a pseudo-plateau of residual pressure at about 280 °C.

Between 315 and 450 °C (region D in Figure 6), a significant increase in the conductivity is observed. A linear temperature dependence of the conductivity is observed, with an activation energy close to 0.4 eV. It should be remarked that this temperature region corresponds to the main contribution to the proton generation following eq 1. However, this step could be regarded as a complicated process in which at least three overlapping reactions could be involved: (i) release of remaining hydroxyl groups belonging to the intercalated Al-polycations, (ii) removal of water molecules originated from the condensation reaction of OH groups from the Al-polyoxyhydroxy species and OH groups located at unshared corners of the octahedra, and (iii) H^+ migration to structural vacant sites in the octahedral silicate sheet. In this temperature range, the weight loss deduced from the TG curves is about 1.6%, and the DSC plots show two endothermic processes at 330 and 420 °C, respectively (Figure 3). Nevertheless, point iii is the most convincing process, as this is the temperature region (300−400 °C) where most IR works of adsorbed pyridine (or other bases) show an important loss of the Brønsted acidity (and sometime total disappearance of the pyridinium band and catalytic activity).[31−35]

Finally, for thermal treatments above 450 °C (region E in Figure 6), a linear Arrhenius plot of the electrical conductivity is observed, with an activation energy of 0.9 eV. This behavior can be ascribed to the mobility of thermally activated ions (mainly naked H^+ ions and, probably also, residual exchangeable cations, e.g. Na^+) present in the PILC galleries. The characteristic dehydroxylation reaction of the silicate taking place above 600 °C, as determined from thermal analyses (Figure 3), does not affect significantly the electrical behavior.

(31) Occelli, M. L.; Lester, J. E. *Ind. Eng. Chem. Prod. R. & D.* **1985**, *24*, 27.
(32) Poncelet, G.; Schutz, A. In *Chemical Reactions in Organic and Inorganic Constrained Systems*; Setton, R. Ed.; Reidel: Dordrecht, 1986; p 145.
(33) Tichit, D.; Fajula, F.; Figueras, F.; Gueguen, C.; Bousquet, J. *Fluid Cracking Catalysts, ACS Symposium Series* **1988**, *375*, 237.
(34) Ko, An-Nan; Chang Hsin-Chuang *J. Chin. Chem. Soc.* **1992**, *39*, 81.
(35) Bradley, S. M.; Kidd, R. A. *J. Catal.* **1993**, *141*, 239.

Table 3. Comparative Results Obtained from Impedance Measurements and Thermal Analyses Applied during the in Situ Formation of Al-PILC Samples

temp range (°C)	impedance measurements	thermal analyses	interpretation
A, 25−100	increase of the semicircle diameter in the Nyquist plots	TG: weight loss (11.6%) DTA and DSC: endo CRTA: increase of residual pressure	proton conductivity decrease due to the loss of adsorbed water molecules acting as carriers for the charged species
B, 100−180	minimum values of the electrical conductivity	TG: weight loss (3%) DTA: endo (160 °C) DSC: endo (170 °C) CRTA: minimum value in the generated pressure (175 °C)	the conductivity remains almost constant at its minimum values due to a nearly total removal of water molecules (mainly H_2O from Al-polycations)
C, 180−315	Increase of conductivity vs temperature following an Arrhenius type behavior ($E_a = 0.2$ eV)	TG: weight loss (1.8%) CRTA: plateau at ∼280 °C	intermediate step mainly ascribed to water loss (OH from Al-polycations) leading to proton generation (eq 1)
D, 315−450	Arrhenius slope change ($E_a = 0.4$ eV)	TG: weight loss (1.6%) DSC: endo (∼330; ∼420 °C) CRTA: decrease of generated pressure (shoulder at ∼430 °C)	proton migration to octahedral vacancies layers (other overlapped processes, as release of remaining OH of Al-polycations, could also take place)
E, 450−850	Arrhenius slope change ($E_a = 0.9$ eV)	TG: weight loss (3.8%) DTA: endo (670 °C) DSC: endo (645 °C) CRTA: decrease of residual pressure	thermally activated mobility of H^+ and residual exchangeable cations (e.g. Na^+)

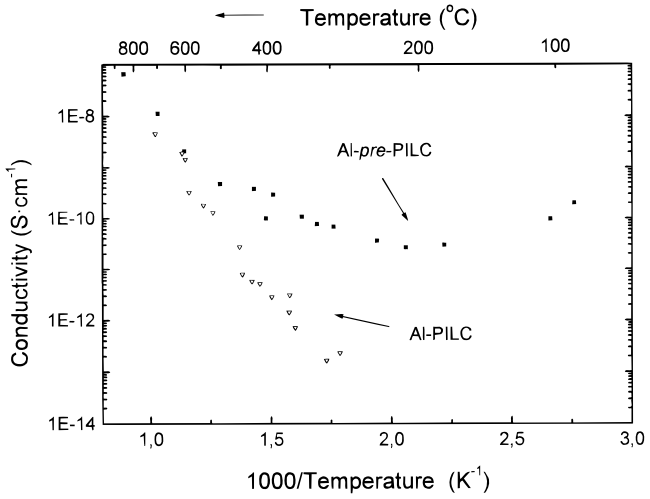

Figure 7. Conductivity values vs temperature for Al-pre-PILC and corresponding Al-PILC.

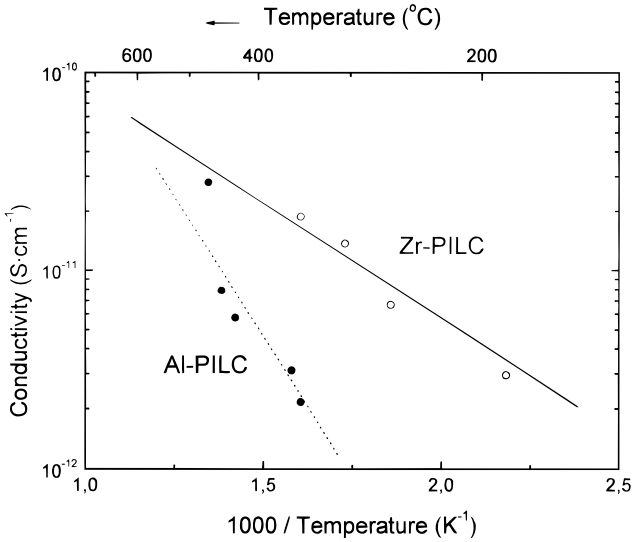

Figure 8. Arrhenius plots of an Al-PILC and a Zr-PILC, prepared with Wyoming montmorillonite (SWy-1).

Table 3 summarizes the main data of the impedance behavior and the interpretation of these results, with regard with the thermal analyses.

In addition to the application of the impedance technique to study the formation mechanism of the PILCs by following the in situ processes accompanying the synthesis of these materials, EIS was used to study the electrical properties of the resulting PILC materials. The impedance behavior of Al-PILCs compared to Al-pre-PILCs during thermal heating are quite different, as is clearly shown in Figure 7. Nevertheless, in both cases the conductivity values are several orders of magnitude greater than in the starting montmorillonite for all the studied temperature domains.[36] After proton migration to the octahedral layers, followed by thermal activation, only naked ions (protons and probably some residual cations) remain in the galleries of the PILCs as electrical charge carriers. Moreover, an increasing fraction of protons could migrate to the octahedral vacancies, favored by the temperature increase. This explains the low conductivity values found for Al-PILCs compared to Al-pre-PILCs. The tendency to reach the same conductivity values at temperatures above 550 °C for both samples (i.e. Al-PILC and Al-pre-PILC) could be an indication of the end of the migration process of the alumina pillar.

The role of the pillar nature on the conductivity has been also studied by comparing the behavior of different series of Zr- and Al-PILCs samples. For Al-PILCs prepared from montmorillonite of different sources, a similar electrical response was always observed (Figure 8). The slope of the Arrhenius plots gave activation energies close to 1.1 eV, for all these Al-PILC samples.

The Zr-PILC sample (Wyoming montmorillonite) shows a different behavior relative to the Al-pillared clay samples (Figure 8). It presents higher proton conductivity values than Al-PILCs, which are also measurable from lower temperatures (>185 °C for Zr-PILCs compared to >300 °C for Al-PILCs). Apparently this behavior could be ascribed to the stronger acidity of Zr-PILCs compared to Al-PILCs. Nevertheless, the interpretation of the strong acidity of Zr-PILCs relative to Al-PILCs is questionable.[37] Zonghui and Sun Guida

(36) Aranda, P.; Galván, J. C.; Casal, B.; Ruiz-Hitzky, E. *Electrochem Acta* **1992**, *37*, 1573.

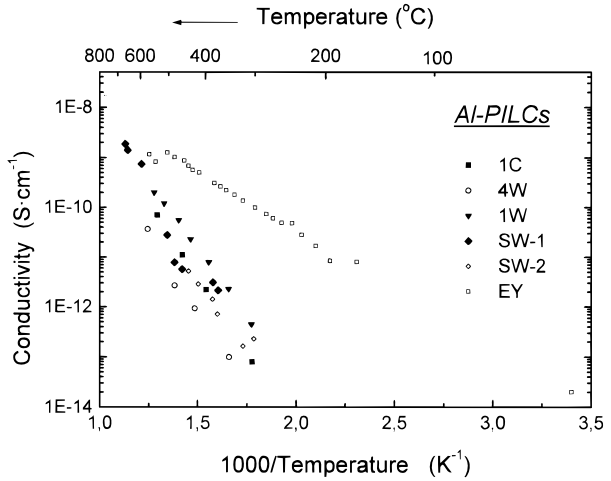

Figure 9. Conductivity vs temperature for Al-PILCs prepared with different smectites: Wyoming montmorillonites (SW-1, SW-2) and acid-activated montmorillonites from Laporte (1C, 1W, 4W) and Yunclillos saponite (EY).

concluded that Zr-PILCs have weak acidity (mainly Lewis).[38] Occelli found that the loss of Brønsted acidity occurs at lower temperature than for Al-PILCs.[31] The behavior observed for Zr-PILCs could indicate an easier migration of the protons. In addition to that, Poncelet[39] has found some evidence that in Zr-PILCs the acidity is mainly associated with the water interacting with the Zr, this being different than the protons generated during the precursor to pillar transformation in Al-PILCs. Impedance measurements carried out to obtain information on the reversibility aspects of the conductivity values, in the temperature domains here studied, show that in contrast to Al-PILCs, Zr-PILCs rehydrate after they have been calcinated at 400−500 °C, and the difference we notice between the two PILCs may due to the water regained by the Zr-PILCs.

To study the role of the clay's nature on the conductivity properties, impedance measurements have been made on montmorillonite- and saponite-based Al-PILCs. The Al-PILCs were prepared with clays from different sources. Some samples were synthesized in our laboratory using Wyoming montmorillonite. Pilot-scale Al-PILCs samples, derived from acid-activated montmorillonites (1C, 1W, 4W) were prepared at the National Technical University of Athens. Figure 9 shows the results of plots of conductivity vs temperature. All of the Al-PILC samples involving montmorillonite clays evolve in a similar way, presenting identical activation energy values. The Al-PILCs prepared with saponite (EY) exhibit higher conductivities (Figure 9) than Al-PILCs obtained from montmorillonite clays, indicating greater H^+ availability. Besides, the Al-pillared saponites have a lower activation energy, 0.45 eV, compared to 1.1 eV found for montmorillonite Al-PILCs. The higher proton conductivity detected in saponite (vs montmorillonite) could be correlated with the higher acidity and higher proton content for the Al-PILC saponite. In agreement with these last results, recent publications[40−45] have reported (i) a greater proton content in Al-PILC saponites relative to pillared montmorillonites, evidenced by the presence of a new OH band at 3595 cm^{-1} ascribed to the Si−O−Al bond opening in the tetrahedral layer (absent in Al-pillared montmorillonites);[46] (ii) a higher catalytic activity of Al-PILC saponite compared with Al-PILC montmorillonites in proton-catalyzed reactions, and (iii) that all Al-pillared clays which have structural substitution in the tetrahedral layers (beidellite, saponite) have higher catalytic activities compared with clays with octahedral structural substitutions. Al-pillared clays prepared with montmorillonites of various origins exhibit similar catalytic activities. Thus, the catalytic data and conductivity differences observed in this study fit in a very interesting way: similar conductivity results for different Al-pillared montmorillonites and higher conductivities for Al-pillared saponites.

Concluding Remarks

Significant changes in the conductivity behavior have been observed by the electrochemical impedance technique during the calcination step of Al-PILCs. These changes are ascribed to the progressive loss of both water molecules and hydroxyl groups from the Al-polyoxyhydroxy cations, which is accompanied by the intracrystalline proton generation detected and evaluated by the impedance method. Thus, this technique allows determination of the temperature range where the H^+ ions are generated, which is of great importance in view of how proton conductivity correlates with the acid catalytic activity inherent in Al-PILCs. In addition, the impedance results combined with those provided by other physicochemical techniques are useful to distinguish the different intermediate steps occurring during the transformation of the Al-polyoxyhydroxy cation species to the alumina pillars, affording information on their formation mechanism. Finally, the second part of this study has shown that the electrochemical impedance technique is also an advantageous tool to evaluate the proton conductivity of PILCs as a function of their intrinsic acidity, which depends on the origin of the starting clays as well as the nature of the pillar.

Acknowledgment. Partial financial support from BRITE-EURAM II (European Union, BR2-CT-94-0629), CICYT (Spain, MAT94-1505-CE, MAT97-1271-CO2, MAT-97-0326), and DGICYT (Spain, EU95-0008) is gratefully acknowledged. We are indebted to Prof. G. Poncelet, Université Catholique de Louvain, Belgium, and to Prof. N. Papayanakos, National Technical University of Athens, Greece, for supplying Al-PILCs samples and for their helpful discussions.

CM980076I

(37) Johnson, J. W.; Brody, J. F.; Soled, S. L.; Gates, W. E.; Robbins, J. L.; Marruchi-Soos, E. *J. Mol. Catal. A* **1996**, *107*, 67.
(38) Zonghui Liu; Sun Guida *Stud. Surf. Sci. Catal.* **1985**, *24*, 493.
(39) Poncelet, G. Personal communication.
(40) Chevalier, S.; Franck, R.; Lambert, J. F.; Barthomeuf, D.; Suquet, H. *Appl. Catal. (A)* **1994**, *110*, 153.
(41) Jiang, D. Z.; Sun, T.; Liu, Z. Y.; Min, E. Z.; He, M. Y. *Chin. J. Chem.* **1993**, *11*, 509.
(42) Moreno, S.; Sun Kou R.; Poncelet, G. *J. Phys. Chem.* **1997**, *101*, 1569.
(43) Moreno, S.; Gutierrez, E.; Alvarez, A.; Papayannakos, N. G.; Poncelet, G *Appl. Catal. (A)* **1997**, *165*, 103.
(44) Moreno, S.; Sun Kou R.; Poncelet G. *J. Catal.* **1996**, *162*, 198.
(45) Molina, R.; Moreno, S.; Vieira-Coelho, A.; Martens, J. A.; Jacobs, P. A.; Poncelet, G. *J. Catal.* **1994**, *148*, 304.
(46) Chevalier, S.; Franck, R.; Suquet, H.; Lambert, J. F.; Bartholomeuf, D. *J. Chem. Soc., Faraday Trans.* **1994**, *90*, 667.